Structural Control of the Electronic Properties of Photodynamic Azobenzene-Derivatized π-Conjugated Oligothiophenes

Bruno Jousselme,[†] Philippe Blanchard,[†] Magali Allain,[‡] Eric Levillain,[†] Marylène Dias,[†] and Jean Roncali[†]*

Groupe Systèmes Conjugués Linéaires, CIMMA, UMR CNRS 6200, Université d'Angers, 2 Bd Lavoisier, 49045 Angers, France, and CIMMA, UMR CNRS 620, Université d'Angers, 2 Bd Lavoisier, 49045 Angers, France

Received: January 13, 2006

Quaterthiophenes containing a median 3,3′-dimethoxybithiophene (**4MTZ**) or bis(3,4-ethylenedioxythiophene) (**4ETZ**) block and an azobenzene group attached at two internal β-positions of the end thiophene rings have been synthesized. The analysis of the crystal structure of the two compounds by X-ray diffraction shows that, for **4MTZ**, the quaterthiophene chain adopts a syn−anti−syn conformation similar to the parent system based on unsubstituted quaterthiophene. In contrast, **4ETZ** presents an all-anti conformation stabilized by noncovalent intramolecular interactions between oxygen atoms and thiophenic sulfur atoms. The effect of the photoisomerization of the azobenzene group on the electronic properties of the attached π-conjugated quaterthiophene chain has been analyzed by UV−vis spectroscopy and cyclic voltammetry. The results obtained for **4MTZ** suggest very limited geometrical changes due to the restricted rotation around the central interannular single bond caused by steric interactions between the methoxy groups. In contrast, upon trans to cis photoisomerization of the attached azobenzene group of **4ETZ**, the quaterthiophene chain undergoes a reversible conformational switch to a final state with a lower HOMO level and a larger HOMO−LUMO gap than the initial state.

Introduction

Motion generation at the molecular level is a focus of considerable current interest from the perspective of developing nanoscale molecular actuators, machines, and motors.[1−7] During the past decade, various prototypes of dynamic molecular architectures such gears[2], shuttles,[3] ratchets,[4] motors,[5] and muscles[6] capable of converting thermal, chemical, or photochemical energy into molecular motion and, hence, mechanical energy, have been reported. Initial prototypes of molecular machines generating a repeatable and directionally controlled motion were essentially powered by means of changes in the oxidation state of a mobile part of the molecular architecture. Thus, Stoddart and co-workers have developed molecular shuttles in which modification of the oxidation state of a redox-active system embedded in a rotaxane induces its translocation along a linear axis.[3a,7] Sauvage and co-workers have synthesized molecular machines and muscles powered by chemically or electrochemically induced changes of the redox state and, hence, coordination sphere of metal complexes in rotaxanes containing tetra- and pentacoordination sites.[3b,c,6]

Among the various possible power sources, photons present the advantages of direct and rapid access to the target active site and absence of chemical reagent. Shinkai and co-workers have synthesized a first generation of photoresponsive dynamic molecular systems where photoisomerization of azobenzene was used to modulate the affinity of macrocyclic crown ethers toward metal cations.[8] Photochemically powered molecular machines undergoing circular motion have been developed by Ferringa et al.[5b,c] Gaub et al. have investigated a polymeric system capable of producing a single-molecule optomechanical cycle,[9] while more recently, Kinbara, Aida and co-workers have synthesized a photoresponsive molecular scissor based on a combination of azobenzene and ferrocene units.[10]

Although the volume change associated with the redox process of conjugated polymers has been used to develop bulk electrochemical actuators,[11] attempts to utilize π-conjugated systems in dynamic molecular systems remain scarce. A first step in this direction was reported by Marsella et al., who investigated poly[cyclooctatetrathiophene] and tetra[2,3-thienylene] as a basic unit for molecular actuation.[12] Recently, we have proposed a different concept in which stimulation of a driving group covalently attached at two fixed points of an oligothiophene chain generates reversible geometrical and dimensional changes in the π-conjugated system.[13] A specific interest of this approach is that the oligothiophene chain simultaneously constitutes the target of the generated motion and an almost ideal optical and redox probe, allowing the real-time monitoring of the chemo- or photomechanically produced molecular motion by simple electrochemical and optical techniques.

This concept was initially demonstrated for crown-annelated oligothiophenes in which molecular motion was produced by metal cation complexation.[13a] More recently, we have described photochemically driven systems in which an azobenzene group attached at two defined points of quarterthiophene (**4TZ**) and sexithiophene (**6TZ**) chains served as a photoactuating governor (Chart 1).[13b,c] The analysis of the photodynamic behavior of these systems by ^{1}H NMR, UV−vis spectroscopy, cyclic voltammetry, and theoretical calculations has shown that trans to cis photoisomerization of the azobenzene generates a conformational switch in the oligothiophene chain that results in an increase of the HOMO level of the π-conjugated system.[13b,c]

We now report the synthesis and photodynamic behavior of two new systems in which the median bithiophenic part of **4TZ**

* Corresponding author. E-mail: jean.roncali@univ-angers.fr.
† Groupe Systèmes Conjugués Linéaires.
‡ CIMMA.

10.1021/jp060254s CCC: $33.50
Published on Web 02/18/2006

CHART 1

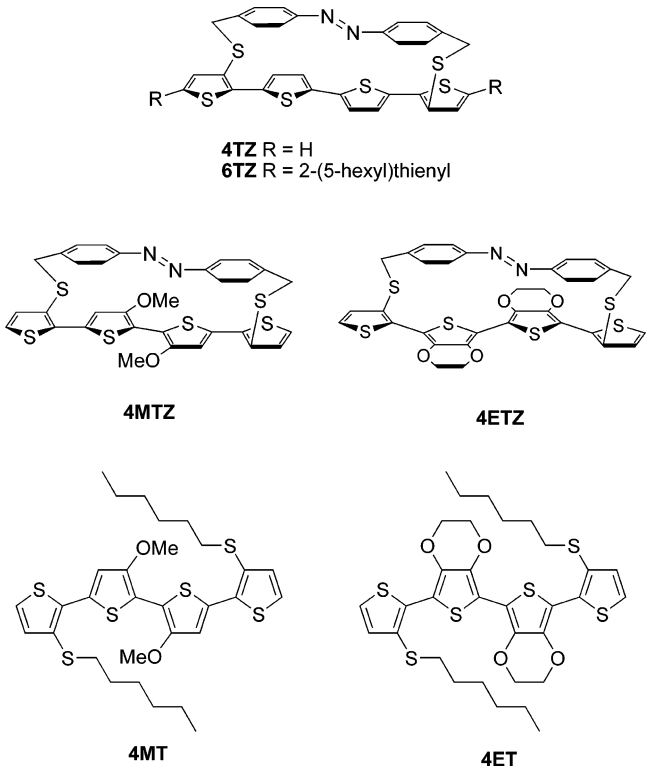

has been replaced by 3,3′-dimethoxybithiophene (**4MTZ**) and bis(3,4-ethylenedioxythiophene) (EDOT) (**4ETZ**). The crystallographic structure of these compounds has been analyzed by X-ray diffraction, and the photomechanically induced modifications of the electronic properties of the quaterthiophene (4T) conjugated system have been investigated by UV−vis spectroscopy and cyclic voltammetry with reference to the model compounds **4MT** and **4ET**.

Results and Discussion

Synthesis. The synthesis of the target compounds is depicted in Scheme 1. Treatment of 3-methoxythiophene and EDOT with *n*-butyllithium, followed by oxidative coupling with copper chloride, gave 2,2′-bi(3-methoxythiophene) **1a** and 2,2′-bi(3,4-ethylenedioxythiophene) **1b**[14] in 34 and 66% yields, respectively. Dilithiation of these two compounds and reaction with tributyltin chloride afforded the bis(tributylstannyl) derivatives **2a** and **2b**. These compounds were immediately subjected to a double Stille coupling reaction with 2-bromo-3-(2-cyanoethylsulfanyl)thiophene **3**[15] by using $Pd(PPh_3)_4$ as a catalyst to give quaterthiophenes **4a** and **4b** with two protected thiolate groups in 49 and 46% yields, respectively. Thiolate deprotection by cesium hydroxide, followed by reaction with *n*-bromohexane, gave the dihexylsulfanyl-substituted quaterthiophenes **4MT** and **4ET** in 53 and 60% yields, respectively. The two target compounds **4MTZ** and **4ETZ** have been prepared in one pot by deprotection of the thiolate groups of **4a** and **4b** by cesium hydroxyde and ring closure by reaction with bis-*p*-bromomethylazobenzene **5**[16] under high dilution conditions, according to the already-reported procedure.[13]

Crystallographic Analysis. Figure 1 shows the crystallographic structure of a single crystal of **4MTZ**. The 4T and azobenzene chains lie in two quasiparallel planes, and the 4T chain adopts an syn−anti−syn (SAS) conformation similarly to the parent system based on a nonsubstituted 4T chain (**4TZ**).[13c] Examination of crystallographic data shows that the

SCHEME 1: Synthesis of 4MTZ and 4ETZ[a]

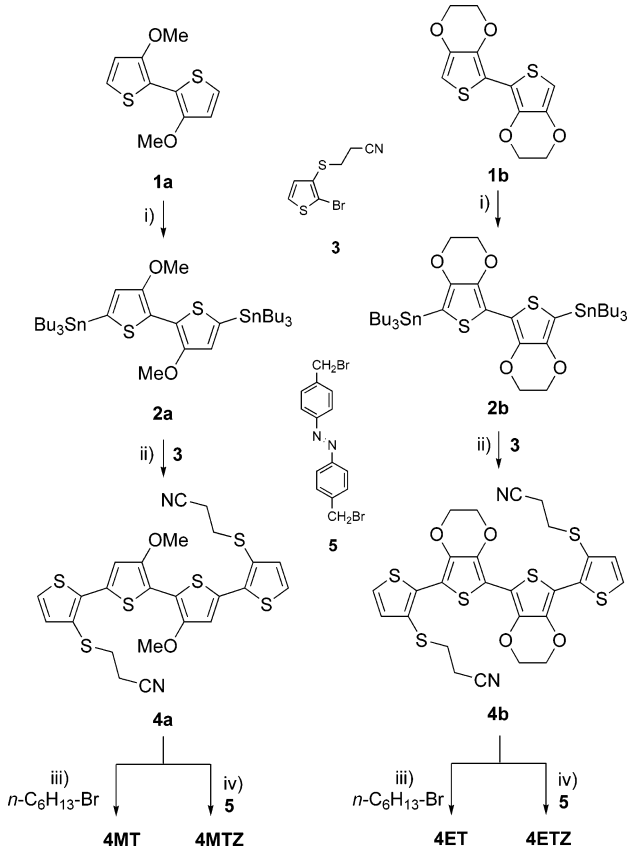

[a] (i) 1. *n*-BuLi, THF, −78 °C. 2. Bu_3SnCl, THF −78 °C. (ii) **3**, $Pd(PPh_3)_4$, Toluene Δ. (iii) 1. $CsOH{\cdot}H_2O$, MeOH, DMF, 20 °C 20 min. 2. *n*-hexylbromide 20 °C 15 h. (iv) 1. $CsOH{\cdot}H_2O$, MeOH, DMF, 20 °C 20 min. 2. **5**, 20 °C high dilution.

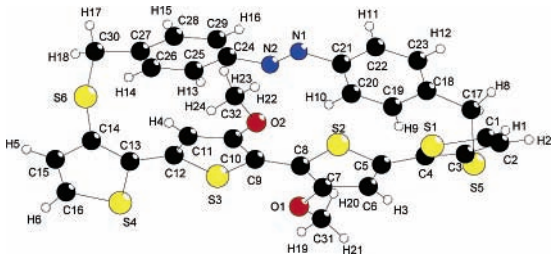

Figure 1. Crystallographic structure of **4MTZ**.

non bonded S···O distances S3−O1 = 2.858(2) Å and S2−O2 = 2.830(2) Å are significantly shorter than the sum of the van der Waals radii of sulfur and oxygen (3.35 Å). These results show that the planar anti conformation of the central dimethoxybithiophene core is stabilized by noncovalent intramolecular interactions. The 12.385(1) Å distance found between the two sulfur atoms serving as anchoring points for the azobenzene group (S5−S6) agrees well with the 12.1 Å distance obtained by geometrical optimization of 3,3‴-dimethylsulfanyl quaterthiophene.[13a]

The crystal structure of **4ETZ** contains two independent molecules that are diastereoisomers (Figure 2). In fact, the last step in the assembling of the molecule leads to two pairs of enantiomers. As shown in Scheme 2, formation of enantiomers is a consequence of the direction of the nucleophilic attack of the dithiolate either above or below the azobenzene core. Then, the spatial arrangement of the free lone pairs of the nitrogen atoms results in the formation of diastereoisomers.

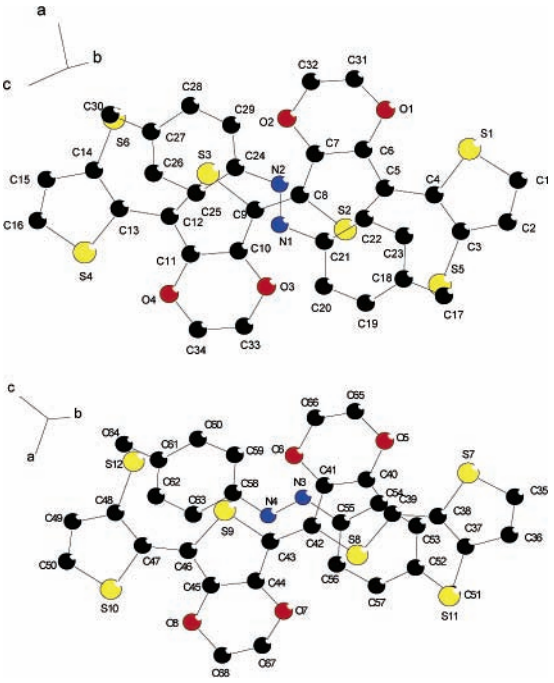

Figure 2. Crystallographic structure of the two stereoisomers of **4ETZ**.

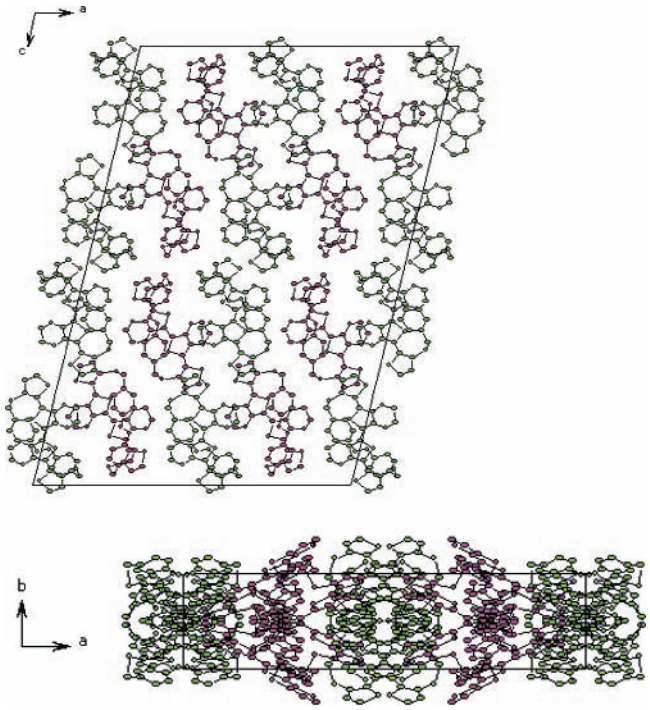

Figure 3. Molecular packing of the two stereoisomers of **4ETZ** in the crystal. Molecule **1** in green and molecule **2** in pink.

Although it is likely that the same process can occur with the other azobenzene-derivatized oligothiophenes, such as **4TZ**, **6TZ**, and **4MTZ**, until now, evidence for the formation of stereoisomers is lacking. In fact, such isomers cannot by distinguished by ^{1}H NMR, while only one isomer was observed in the crystallographic structure.

The molecular packing of **4ETZ** shows that columns of stereoisomers 1 and 2 alternate along the *c* axis (Figure 3). In sharp contrast with **4MTZ** and the other azobenzene-derivatized oligothiophenes that present a syn−anti−syn conformation (SAS),[13b,c] **4ETZ** adopts a fully anti conformation (AAA) (Figure 2). As for **4MTZ**, the nonbonded S···O distances, S1−O1 = 2.78(4) Å, S2−O3 = 2.94(2) Å, S3−O2 = 2.89(2) Å, S4−O4 = 2.81(5) Å, are much shorter than the sum of the van der Waals radii of sulfur and oxygen (3.35 Å).

These results show that, similarly to many conjugated systems containing the EDOT unit, the planar AAA conformation of **4ETZ** is self-rigidified by intramolecular noncovalent interactions between the oxygen atoms of EDOT and the sulfur atom of the adjacent thiophene ring.[17] A noticeable effect of this self-rigidification of the 4T chain in a planar AAA conformation is that the distance between the sulfur atoms of the two sulfide groups serving as fixation sites for the azobenzene group decreases from 12.38 Å for **4MTZ** to ca. 10.90 Å for **4ETZ**. Again, this value agrees well the distance calculated for the optimized AAA conformation of 3,3‴-dimethylsulfanyl quaterthiophene (10.80 Å).[13a]

As a consequence of this shorter S···S distance, the azobenzene group in **4ETZ** is submitted to a stronger constraint than in **4TZ** and **4MTZ**. Whereas, for these latter molecules, part of the constraint is released through a forced rotation of thiophene units, leading to a SAS conformation, for **4ETZ**, the

SCHEME 2: Formation of Stereoisomers during the Synthesis of Azobenzene−Oligothiophene Cyclophanes

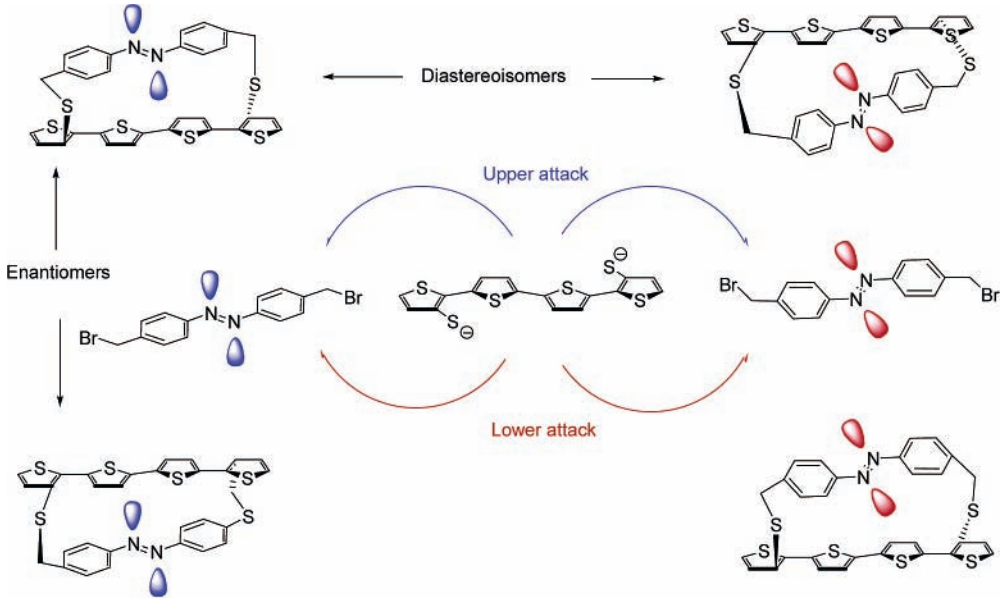

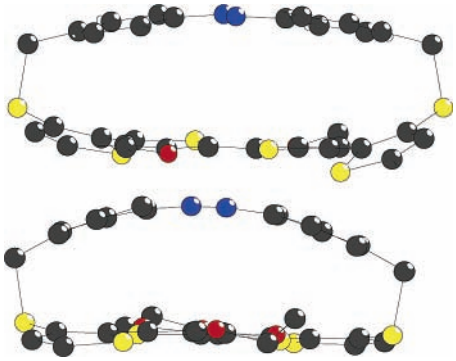

Figure 4. Side view of **4MTZ** (top) and **4ETZ** (bottom) (hydrogen atoms omitted for clarity).

TABLE 1: UV−Vis Spectroscopic Absorption Maxima (in nm) for Compounds 4MTZ and 4ETZ and Their Respective Reference Compounds 4MT and 4ET in Methylene Chloride

compd	4T chain	azobenzene
DMeZ		335, 439
4MT	436	
4MTZ	450	353, 368
4MTZ[a]	446	354, 369
4ET	411, 433, 460	
4ETZ	421, 446, 474	350, 364
4ETZ[a]	416, 432, 460	345, 368
4ETZ[a,b]	410	320, 330

[a] After 5 h irradiation with monochromatic light at 360 nm. [b] Isolated by HPLC.

whole constraint is supported by the azobenzene group, which results in a bending of its geometry (Figure 4).

Optical and Photodynamic Properties. To evidence the effects of the forced interactions between the azobenzene and 4T conjugated systems when assembled into a cyclophane structure, Table 1 lists the UV−vis absorption data for **4MTZ** and **4ETZ** and for the model compounds of their constitutive parts, namely **4MT**, **4ET**, and *p*-dimethylazobenzene (**DMeZ**). The UV−vis spectrum of **4MT** (see Supporting Information) exhibits a broad absorption band with a maximum at 436 nm. In contrast, the spectrum of **4ET** presents a well-resolved vibronic fine structure with three maxima at 411, 433, and 460 nm. As for many EDOT-containing systems, these spectral features typical for rigid conjugated systems result from the already-discussed noncovalent intramolecular S···O interactions.[17] The spectrum of **DMeZ** shows a main absorption band at 335 nm, associated with a $\pi-\pi^*$ transition, and a weak band at 439 nm, corresponding to a $n-\pi^*$ transition. Comparison of these data to those of the 4T and azobenzene parts in compounds **4MTZ** and **4ETZ** reveals several noticeable differences. For **4MTZ**, the λ_{max} of the 4T chain shifts bathochromically from 436 to 450 nm, while the absorption band of the azobenzene group undergoes a red-shift and splits into two subcomponents at 353 and 368 nm. Similar effects are observed for **4ETZ** for which the three maxima of the 4T chain shift bathochromically by 10−14 nm. These modifications of the optical features of both constitutive parts of **4MTZ** and **4ETZ** can be attributed to through-space interactions between the 4T and azobenzene conjugated systems when covalently assembled into a cofacial structure. As already observed for **4TZ** and **6TZ**, the presence of the attached azobenzene group results in a strong quenching of the photoluminescence of the 4T chain.[13]

The photodynamic behavior of **4MTZ** and **4ETZ** has been analyzed by recording their UV−vis spectrum under continuous monochromatic irradiation at 360 nm. A control experiment

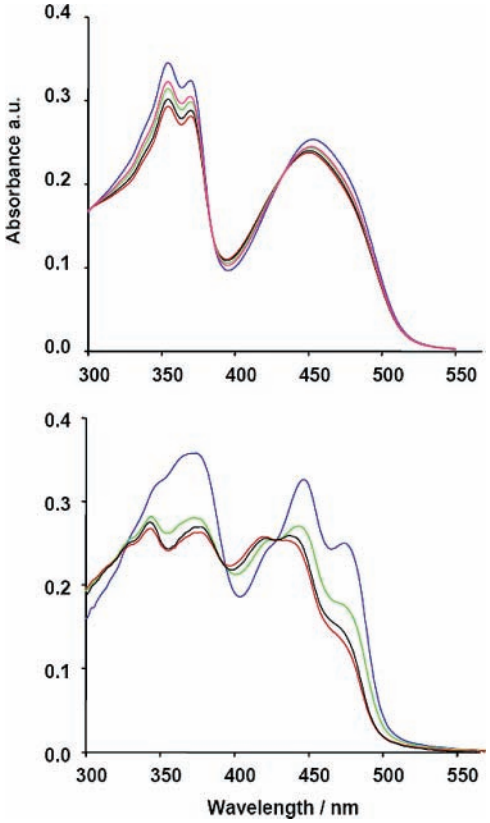

Figure 5. Photomechanically induced changes in the UV−vis spectrum of **4MTZ** (2.0×10^{-5} M in CH_2Cl_2) (top) and **4ETZ** (1.5×10^{-5} M in CH_2Cl_2) (bottom). Blue: initial state; red: after 5 h monochromatic irradiation at 340 nm.

showed that, as expected, irradiation of a 10^{-4} M solution of *p*-dimethylazobenzene **DMeZ** leads to the bleaching of the $\pi-\pi$ transition with a blue-shift of λ_{max} to 305 nm and a slight intensification of the $n-\pi^*$ transition at 439 nm. As it appears in Figure 5, irradiation of **4MTZ** under the same conditions produces a small decrease of the intensity of the azobenzene absorption band, while that of the quaterthiophene chain undergoes a small blue-shift and a slight decrease in intensity. The small magnitude of these spectral changes suggests that, in **4MTZ**, the 4T chain undergoes only limited geometrical modifications. In fact, the analysis of the dynamic process by ^{1}H NMR according to the already-described procedure[13b,c] shows that, after 5 h of irradiation, photoconversion is limited to ca. 10%, while 47% of conversion was reached for **4TZ** under the same conditions.[13b,c]

The initial spectrum of **4ETZ** shows a first band with two subcomponents at 350 and 364 nm, corresponding to the absorption of the azobenzene group, and a second broad band with two maxima at 446 and 474 nm and a shoulder at 421 nm, corresponding to the absorption of the 4T chain. Monochromatic irradiation of the azobenzene group leads to a decrease of the intensity of the azobenzene band with an enhancement of the resolution of the spectrum. Concurrently, the intensity of the two absorption bands of the 4T chain at 446 and 472 nm also decreases, while the intensity of the 420 nm band increases. These changes in the spectrum of the 4T chain occur around two isosbestic points at 395 and 427 nm. The spectra in Figure 5 correspond to the mixture of the trans and cis forms of **4ETZ**, representing the quasistationary state reached after 5 h of irradiation. As shown by ^{1}H NMR data, this state corresponds to 25% of photoconversion. To gain more information on the spectral features of the pure final photomechanically produced

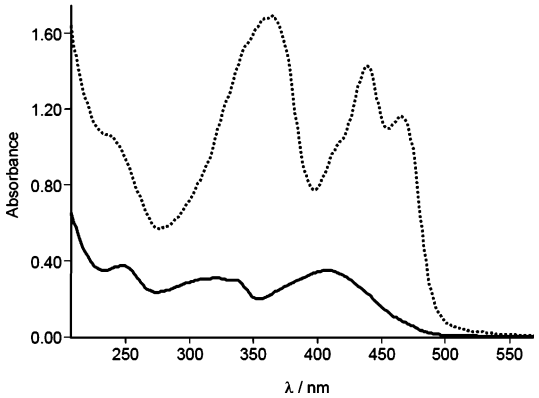

Figure 6. UV−Vis absorption spectra of the two forms of **4ETZ** separated by HPLC in CH_2Cl_2. Dotted line: initial spectrum; solid line: spectrum of the photogenerated twisted form.

form of **4ETZ**, the initial and photoconverted forms of **4ETZ** have been separated by HPLC. As shown in Figure 6, the spectrum corresponding to the nonconverted molecule is, as expected, identical to that of the initial spectrum in Figure 5. On the other hand, the spectrum of the final state shows an absorption band around 330 nm, corresponding to the azobenzene group, and a broad structureless absorption band with a maximum at 410 nm, corresponding to the final geometry of the 4T chain. Comparison of the initial and final spectrum shows that the λ_{max} of both the azobenzene and 4T systems has undergone a considerable hypsochromic shift (ca. 30 nm for the 4T chain).

The contrasting photodynamic behaviors of **4MTZ** and **4TEZ** must be discussed in relation with the chemical structure of the 4T chain and its implication for the geometry of the initial and final states. As already discussed, in every case, the final state of the 4T chain must adopt an ASA conformation in order to accommodate the decrease of the distance between the anchoring sulfur atoms produced by the photoisomerization of azobenzene. For both molecules, conformational transition toward the final ASA geometry implies rotation of one of the two inner thiophene rings relative to the other (in fact, owing to the initial *SAS* geometry of **4MTZ**, the transition should also involve rotation of an outer thiophene ring). On this basis, the different photodynamic behaviors of **4MTZ** and **4ETZ** can be related to differences in the possibilities of rotation around the central single bond. For **4MTZ**, such a rotation is restricted by steric interactions between the methoxy groups. In contrast, for **4ETZ**, incorporation of the two facing alkoxy groups in their respective ethylenedioxy bridges reduces steric hindrance, thus giving a larger degree of freedom around the median single bond. Such effects of reduction of steric hindrance by bridging have been previously demonstrated in the case of 3,4-dimethylthiophene.[18]

Although this reduced steric hindrance opens larger possibilities of rotation around the median single bond, a fully coplanar syn conformation of the two median EDOT rings cannot be reached due to steric interactions between the ethylenedioxy groups, and the persistence of a torsion angle between the two median thiophene rings in the final state can explain the blue-shift of the λ_{max} of the 4T chain after photoconversion of **4ETZ**. Finally, it must be underlined that, in addition to these purely geometrical effects, the two EDOT units confere stronger donor properties on the hybrid 4T chain. Consequently, the decrease of the through-space interactions with the azobenzene group consecutive to the trans to cis isomerization of the latter can be expected to also contribute to a blue-shift of the band maxima. This effect is, in fact, the reverse of that observed when the azobenzene and the 4T systems are brought nearer into a cyclophane-like structure. Finally, it is worth noting that, similarly to the previously described **4TZ** and **6TZ**, the conversion process is fully reversible and the initial spectrum is recovered after irradiation with 480 nm light.

TABLE 2: Cyclic Voltammetric Data Recorded in 0.10 M Bu_4NPF_6/CH_2Cl_2, Scan Rate 100 mV s^{-1}, Ref Ag·AgCl

compd	$E_{pa}1$ (V)	$E_{pa}2$ (V)
4MT	0.60	0.91
4MTZ	0.60	1.19
4MTZ[a]	0.60	1.19
4ET	0.60	0.94
4ETZ	0.60	1.23
4ETZ[a]	0.70	0.99

[a] After 5 h monochromatic irradiation at 360 nm

To summarize, these results show that, in contrast to the parent systems based on unsubstituted oligothiophenes **4TZ** and **6TZ** for which the photoinduced conformational switch results in a decrease of the HOMO−LUMO gap of the oligothiophene chain, the photomechanical conversion of **4ETZ** leads to a final state in which the oligothiophene presents a larger HOMO−LUMO gap.

Electrochemical Behavior. The electrochemical properties of **4MTZ** and **4ETZ** have been analyzed by cyclic voltammetry before and after photoirradiation. Table 2 lists the CV data of the two molecules, together with data for the model compounds **4MT** and **4ET**. The CV of **4MT** and **4ET** (see Supporting Information) shows two reversible one-electron oxidation processes, with anodic peak potentials $E_{pa}1$ and $E_{pa}2$ around 0.60 and 0.91−0.94 V, respectively, corresponding to the successive generation of the cation radical and dication of the 4T chain. Comparison of the CV data for **4MTZ** and **4ETZ** to those of **4MT** and **4ET** shows that, while $E_{pa}1$ is not affected by the fixation of the azobenzene group, $E_{pa}2$ shifts toward positive potentials by 0.28 and 0.29 V for **4MTZ** and **4ETZ**, respectively.

A possible cause for this phenomenon could involve the development of repulsive Coulombic interactions between the electron-deficient azobenzene group and the cation radical of the 4T chain. The fact that such effects were not observed for **4TZ** and **6TZ** suggests that, for **4MTZ** and **4ETZ**, the strong electron donor methoxy and ethylenedioxy groups contribute to localize the positive charge in the middle of the molecule where it can interact with the azobenzene group, which is not the case when the charge is expected to localize on the terminal thiophenes as in **4TZ**.[19]

After photoirradiation, the CV of **4MTZ** remains practically unchanged, confirming in agreement with optical data, that the 4T chain does not undergo significant conformational change. In contrast, the CV of **4ETZ** shows a positive shift of $E_{pa}1$ from 0.63 to 0.70 V and the emergence of a new reversible redox system with an anodic peak potential at 0.99 V (Figure 7).

In the case of **4TZ**, the CV recorded after photoirradiation exhibited a new redox system at less positive potential due to an increase of the HOMO level of the 4T chain. The opposite behavior observed here for **4ETZ** can be attributed to the already-discussed steric hindrance to coplanarity of the two inner thiophene rings in the final ASA conformation (Scheme 3). On the other hand, the negative shift of $E_{pa}2$ can be attributed to two causes. The first involves a decrease of the aleady-discussed through-space interactions between the 4T cation radical and the azobenzene group due to the increased distance between the two systems after photoisomerization.

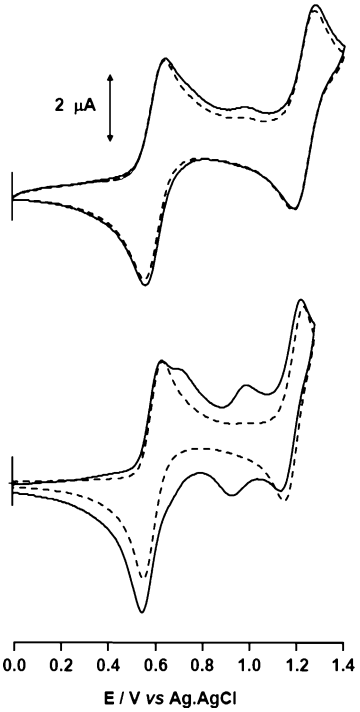

Figure 7. Cyclic voltammograms recorded in 0.10 M Bu_4NPF_6/CH_2Cl_2, scan rate 100 mV s^{-1}. Top **4MTZ**, bottom **4ETZ** ca. 10^{-4} M. Dotted line: initial CV; solid line: after 5 h irradiation with 360 nm monochromatic light.

The second is related to the specificity of the oxidation process of π-conjugated systems with a nondegenerate ground state. In such systems, formation of the cation radical is accompanied by a transition from an aromatic to a quinoid structure.[20] Consequently, when the system is oxidized into the cation radical state, it becomes locked into a defined conformation. Thus, once the conformation of the 4T chain of **4ETZ** has been photomechanically converted from an AAA to an ASA one (at the eventual cost of some deformation of some thiophene cycles[21]), further oxidation to the dication state is expected to be easier than for that of a cation radical still in the initial AAA conformation (Scheme 3). In fact, such a negative shift of the second oxidation potential has been already observed for crown-annelated oligothiophenes on which the ASA conformation of the cation radical was imposed by metal cation complexation.[13a]

Conclusion

Oligothiophene-based photoactuators with an azobenzene group attached at the internal β-position of the end thiophene rings and containing a dimethoxybithiophene and a bi-EDOT median block have been synthesized. X-ray diffraction studies have shown that, whereas for **4MTZ**, the quaterthiophene chain presents a SAS conformation similar to the parent system based on unsubstituted quaterthiophene, **4TEZ** adopts a fully anti conformation stabilized by noncovalent intramolecular sulfur−oxygen interactions.

The photomechanically induced modifications of the electronic properties of the quaterthiophene chain have been investigated by UV−vis spectroscopy and cyclic voltammetry. The results have shown that photoirradiation of the attached azobenzene group of **4MTZ** produces only limited conformational changes due to steric hindrance in the 3,3′-dimethoxybithiophene median core. On the other hand, replacement of 3,3′-dimethoxybithiophene by bi-EDOT brings more freedom to the system, thus allowing reversible geometrical changes of larger magnitude. However, steric interactions between the EDOT rings in the final state lead to a larger HOMO−LUMO gap and a lower HOMO energy level than that of the initial one. These results thus nicely complete the previously reported ones, and they show that the manipulation of the chemical constitution of the π-conjugated system allows development of reversible photodynamic molecular architectures in which the electronic properties of the photomechanically generated final state can be controlled by design in order to reach at will a smaller or a larger HOMO−LUMO gap. Thus, besides providing additional tools for the development of dynamic molecular devices such as actuators or machines, these results open interesting perspectives in the field of organic (opto)electronic devices with the possibility of developing stimuli-responsive organic semiconductors based on functional π-conjugated systems.

Supporting Information Available: Experimental procedure for the synthesis of all compounds. UV−vis spectra and

SCHEME 3

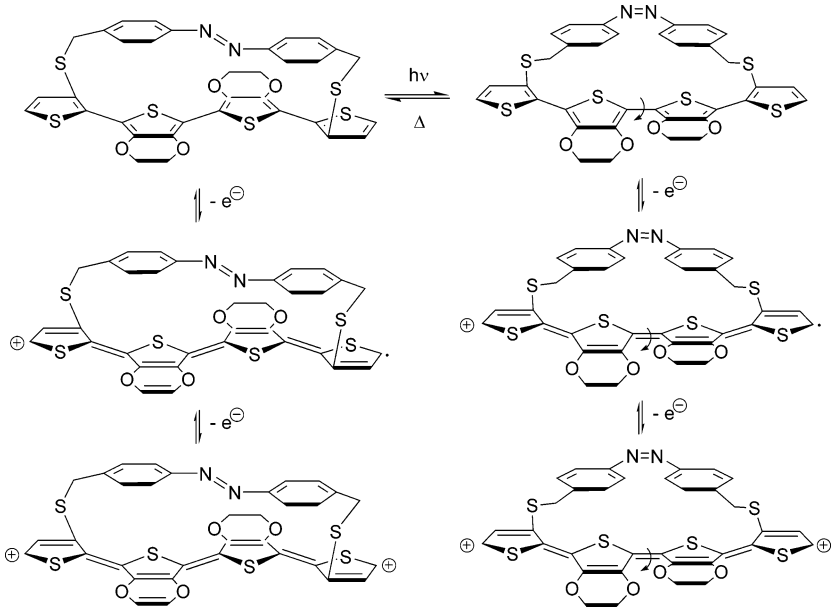

cyclic voltammograms of **4MT** and **4ET**. Crystallographic data, tables of bond distances and angles, positional parameters, and general displacement parameters for **4MTZ** and **4ETZ**. This information is available free of charge via the Intertnet at http://pubs.acs.org.

References and Notes

(1) (a) Drexler, K. E. *Nanosystems: Molecular Machinery, Manufacturing, and Computation*; Wiley: New York, 1992. (b) Special Issue. Movement: Molecular to Robotic. *Science* **2000**, *288*, 79. (c) Balzani, V.; Credi, A.; Raymo, A. F. M.; Stoddardt, J. F. *Angew. Chem., Int. Ed*. **2000**, *39*, 3348. (d) Kinbara, K.; Aida, T. *Chem. Rev.* **2005**, *105*, 1377.

(2) Clayden, J.; Pink, J. H. *Angew. Chem., Int. Ed.* **1998**, *110*, 2040.

(3) (a) Bissell, R. A.; Cordova, E.; Kaifer, A. E.; Stoddardt, J. F. *Nature* **1994**, *369*, 133. (b) Livoreil, A.; Dietrich-Buchecker, C. O.; Sauvage, J.-P. *J. Am. Chem. Soc.* **1994**, *116*, 9399. (c) Sauvage, J.-P. *Acc. Chem. Res.* **1998**, *31*, 611.

(4) Kelly, T. R.; De Silva, H.; Silva, R. A. *Nature* **1999**, *401*, 150.

(5) (a) Kottas, G. S.; Clarke, L. I.; Horinek, D.; Michl, J. *Chem. Rev.* **2005**, *105*, 1281. (b) Koumura, N.; Zijlstra, R. W.; van Delden, R. A.; Harada, N.; Feringa, B. L. *Nature* **1999**, *401*, 152. (c) Pletcher, S. P.; Dumur, F.; Pollard, M.; Feringa, B. L. *Science* **2005**, *310*, 80.

(6) Jimenez, M. C.; Dietrich-Buchecker, C.; Sauvage, J.-P.; DeCian, A. *Angew. Chem., Int. Ed.* **2000**, *39*, 1295.

(7) Fyfe, M. C. T.; Stoddart, J. F. *Acc. Chem. Res.* **1997**, *30*, 393.

(8) (a) Shinkai, S.; Nakaji, T.; Nishiga, Y.; Ogawa, T.; Manabe, O. *J. Am. Chem. Soc*. **1980**, *102*, 5860. (b) Shinkai, S.; Nakaji, T.; Ogawa, T.; Shigematsu, K.; Manabe, O. *J. Am. Chem. Soc*. **1981**, *103*, 111.

(9) Hugel, T.; Holland, N. B.; Cattani, A.; Moroder, L.; Markus, S.; Gaub, H. E. *Science* **2002**, *296*, 1103.

(10) Muraoka, T.; Kinbara, K.; Kobayashi, Y.; Aida, T. *J. Am. Chem. Soc*. **2003**, *125*, 5612.

(11) (a) Baughman, R. H. *Synth. Met.* **1996**, *78*, 339. (b) Smela, E. *Adv. Mater*. **2003**, *15*, 481.

(12) (a) Marsella, M. J.; Reid, R. J. *Macromolecules* **1999**, *32*, 5982. (b) Marsella, M. J.; Reid, R. J.; Estassi, S.; Wang, L.-S. *J. Am. Chem. Soc.* **2002**, *124*, 12507.

(13) (a) Jousselme, B.; Blanchard, P.; Gallego-Planas, N.; Delaunay, J.; Allain, M.; Richomme, P.; Levillain, E.; Roncali, J. *J. Am. Chem. Soc.* **2003**, *125*, 1363. (b) Jousselme, B.; Blanchard, P.; Gallego-Planas, N.; Delaunay, J.; Allain, M.; Richomme, P.; Levillain, E.; Roncali, J. *J. Am. Chem. Soc.* **2003**, *125*, 2888. (c) Jousselme, B.; Blanchard, P.; Gallego-Planas, N.; Levillain, E.; Delaunay, J.; Allain, M.; Richomme, P.; Roncali, J. *Chem. Eur. J.* **2003**, *9*, 5297.

(14) Akoudad, S.; Roncali, J. *Synth. Met.* **1998**, *93*, 111.

(15) (a) Blanchard, P.; Jousselme, B.; Frère, P.; Roncali, J. *J. Org. Chem.* **2002**, *67*, 3961. (b) Van Hal, P. A.; Beckers, E. H. A.; Meskers, S. C. J.; Janssen, R. A. J.; Jousselme, B.; Roncali, J. *Chem. Eur. J.* **2002**, *8*, 5415.

(16) Teren'tev, A. P.; Mogilyanski, Y. D. *Dokl. Akad. Nauk. SSSR* **1955**, 10391.

(17) Roncali, J.; Blanchard, P.; Frère, P. *J. Mater. Chem*. **2005**, *15*, 1589.

(18) Roncali, J.; Garnier, F.; Garreau, R.; Lemaire, M. *J. Chem. Soc., Chem. Commun*. **1987**, 1500.

(19) Akoudad, S.; Frère, P.; Mercier, N.; Roncali, J. *J. Org. Chem*. **1999**, *64*, 4267.

(20) (a) Brédas, J.-L.; Thémans, B. Fripiat, J. G.; André, J. M.; Chance, R. R. *Phys. Rev. B* **1984**, *29*, 6761. (b) Patil, A. O.; Heeger, A. J.; Wudl, F. *Chem. Rev.* **1988**, *88*, 183.

(21) Barbarella, G.; Zambianchi, M.; Bongini, A.; Antolini, L. *Adv. Mater*. **1993**, *5*, 834.